metals

MDPI

Article

Modification Mechanism of Spinel Inclusions in Medium Manganese Steel with Rare Earth Treatment

Zhe Yu [1,2] and Chengjun Liu [1,2,*]

[1] Key Laboratory for Ecological Metallurgy of Multimetallic Ores (Ministry of Education), Shenyang 110819, China
[2] School of Metallurgy, Northeastern University, Shenyang 110819, China
* Correspondence: liucj@smm.neu.edu.cn; Tel.: +86-138-9885-0333

Received: 7 July 2019; Accepted: 19 July 2019; Published: 21 July 2019

Abstract: In aluminum deoxidized medium manganese steel, spinel inclusions are easily to form during refining, and such inclusions will deteriorate the toughness of the medium manganese steel. Rare earth inclusions have a smaller hardness, and their thermal expansion coefficients are similar to that of steel. They can avoid large stress concentrations around inclusions during the heat treatment of steel, which is beneficial for improving the toughness of steel. Therefore, rare earth Ce is usually used to modify spinel inclusions in steel. In order to clarify the modification mechanism of spinel inclusions in medium manganese steel with Ce treatment, high-temperature simulation experiments were carried out. Samples were taken step by step during the experimental steel smelting process, and the inclusions in the samples were analyzed by SEM-EDS. Finally, the experimental results were discussed and analyzed in combination with thermodynamic calculations. The results show that after Ce treatment, the amount of inclusions decrease, the inclusion size is basically less than 5 μm, and the spinel inclusions are transformed into rare earth inclusions. After Ce addition, Mn and Mg in the spinel inclusions are first replaced by Ce, and the spinel structure is destroyed to form $CeAlO_3$. When the O content in the steel is low, S in the steel will replace the O in the inclusion, and $CeAlO_3$ and spinel inclusions will be transformed into Ce_2O_2S. By measuring the total oxygen content of the steel, the total Ce content required for complete modification of spinel inclusions can be obtained. Finally, the critical conditions for the formation and transformation of inclusions in the Fe-Mn-Al-Mg-Ce-O-S system at 1873K were obtained according to thermodynamic calculations.

Keywords: medium manganese steel; spinel inclusions; Ce treatment; modification mechanism

1. Introduction

Medium manganese steel is a typical representative of third generation automotive steel with high strength and high plasticity. It can be applied to many body structure parts including automobile A-pillars, B-pillars, anticollision beams, and sill reinforcement. Industrial experimental studies have shown that (Mn,Mg)O·Al_2O_3- and MgO·Al_2O_3-type spinel inclusions will form during refining of aluminum deoxidized medium manganese steel [1]. Spinel inclusions are generally angular and have high hardness, which is the main cause of stamping and cracking defects in automotive steel [2,3]. Therefore, it is necessary to modify the spinel inclusions to improve the toughness of medium manganese steel. At present, low-melting CaO-MgO-Al_2O_3 inclusions obtained by calcium treatment are generally expected to avoid the damage of hard inclusions [4,5]. However, large-size inclusions cannot be completely modified due to kinetic conditions, which means that the spinel phase core of the complex inclusions will still exist and be exposed after rolling [6].

The rare earth element Ce has a good modification effect on the spinel [7–9], which can modify the hard oxide inclusions into rare earth inclusions with a soft hardness [10]. Huang et al. [7,9]

and Wang et al. [8] respectively studied the modification behavior of Ce on inclusions in drill steel and high-speed railway steel, and the transformation mechanism of spinel to Ce_2O_3 and Ce_2O_2S was described. However, there are relatively few reports on rare earth modified spinel inclusions. The modification mechanism of Ce on the spinel inclusions is not comprehensive, and the effect of aluminum content on Ce treatment has not been reported. Therefore, in this paper, the modification behaviors of spinel inclusions after Ce treatment in medium manganese steel with different aluminum contents were studied. Meanwhile, the Ce content required for complete modification of spinel inclusions was discussed in combination with thermodynamic calculations, which are intended to guide the appropriate addition of rare earth in the actual production process.

2. Experimental Procedure

High-temperature simulation experiments were carried out by using a $MoSi_2$ furnace (TianJin Muffle Technology Co. Ltd, Tianjin, China). According to the general composition of medium manganese steel, the target Al content was set to three levels: low aluminum (0.02%), numbered R1; medium aluminum (0.2%), numbered R2; and high aluminum (2.0%), numbered R3. The experimental steps are as follows. Approximately 400 g of pure iron and an MnFe alloy was placed in a corundum crucible and then placed in the constant temperature zone of the furnace. The master irons (pure iron and MnFe alloy) were heated to 1873 K under argon atmosphere with a flow rate of 0.4 L min^{-1}. Subsequently, the oxygen activity in the molten steel was measured by an electrolyte oxygen probe, and it was defined as the initial oxygen activity (No. 1 $a_{[O]}$). Based on the target Al content, a certain amount of Al wire was added, and NiMg alloy was added 10 min later. No. 2 $a_{[O]}$ was measured by electrolyte oxygen probe after another 10 min from the addition of NiMg alloy, and then sample 0 was taken by a quartz tube and quenched in an ice bath. Finally, CeFe alloy was added into the molten steel to modify inclusions. Thereafter, the molten steel was respectively held for 1, 10, and 30 min at 1873 K (1600 °C) and then successively sampled as above (sample 1–sample 3). After taking sample 2, the oxygen activity was measured by an electrolyte oxygen probe, which was defined as the final oxygen activity (No. 3 $a_{[O]}$). The experimental process is provided in Figure 1. Table 1 shows the compositions of raw materials, including pure iron, MnFe alloy, Al wire, NiMg alloy, and CeFe alloy.

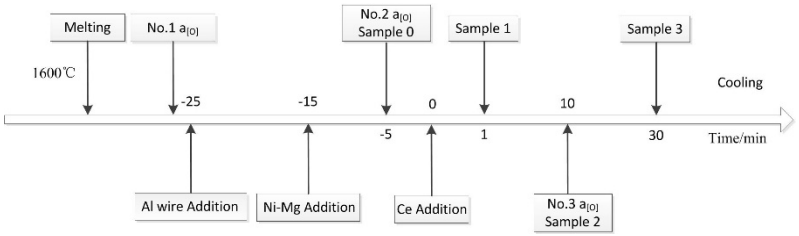

Figure 1. Schematic diagram of the experimental process.

Table 1. Chemical composition of raw materials (mass fraction/%).

Type	Fe	Ni	Mg	Al	C	Si	Mn	Ce	S	P	Others
Pure iron	99.9	0.01	-	0.001	0.0021	0.01	0.03	-	0.003	0.005	0.03
Al wire	-	-	-	99.99	-	-	-	-	-	-	0.01
MnFe alloy	12.57	-	-	-	1.5	1.5	84.2	-	0.03	0.2	-
NiMg alloy	0.93	80.12	17.98	-	0.78	0.19	-	-	-	-	-
CeFe alloy	79	-	-	-	-	-	-	19	-	-	2

To observe inclusions of steel, the steel samples were polished by SiC paper and diamond suspensions. The chemical compositions and morphology of inclusions were analyzed through a scanning electron microscope (SEM, Phenom Prox, Eindhoven, The Netherlands) and an energy dispersive spectroscope (EDS, Phenom Prox, Eindhoven, The Netherlands). The contents of aluminum, manganese, magnesium, and cerium in the steel were determined by using an inductively coupled

plasma optical emission spectrometer (ICP-OES, PerkinElmer, Waltham, MA, USA). The content of sulfur was measured by a carbon and sulfur analyzer. The total oxygen content was measured by an oxygen and nitrogen analyzer. The contents of each element in the three steels (numbered R1, R2, and R3) are listed in Table 2.

Table 2. Chemical composition of experimental steels (mass fraction/%).

No.	C	Mn	Al	Mg	Ce	S	$a_{[O]}$			TO
							No. 1	No. 2	No. 3	
R1	0.23	8.95	0.019	0.001	0.014	0.016	0.0149	0.0014	0.0005	0.0045
R2	0.21	9.18	0.21	0.001	0.015	0.016	0.0124	0.0002	0.0002	0.0021
R3	0.25	9.35	2.03	0.002	0.013	0.014	0.0149	0.0001	0.0001	0.0006

3. Results

3.1. Inclusion Transformation

The types of typical inclusions in the experimental steel are shown in Figure 2; there are five types in common. The type 1 inclusions are Al_2O_3, as shown in Figure 2a. Almost no obvious Mn element was detected in this type of inclusion. Both the type 2 and type 3 are spinel inclusions, namely (Mn,Mg)O·Al_2O_3 and MgO·Al_2O_3 spinel, respectively. The type 4 and type 5 inclusions are rare earth inclusions, and they appear bright white under SEM backscatter conditions. The type 4 inclusions are $CeAlO_3$, which are mostly block-shaped and have a small size of about 2~5 μm. The type 5 inclusions are Ce_2O_2S, which are mostly spherical and have a size of about 3~8 μm.

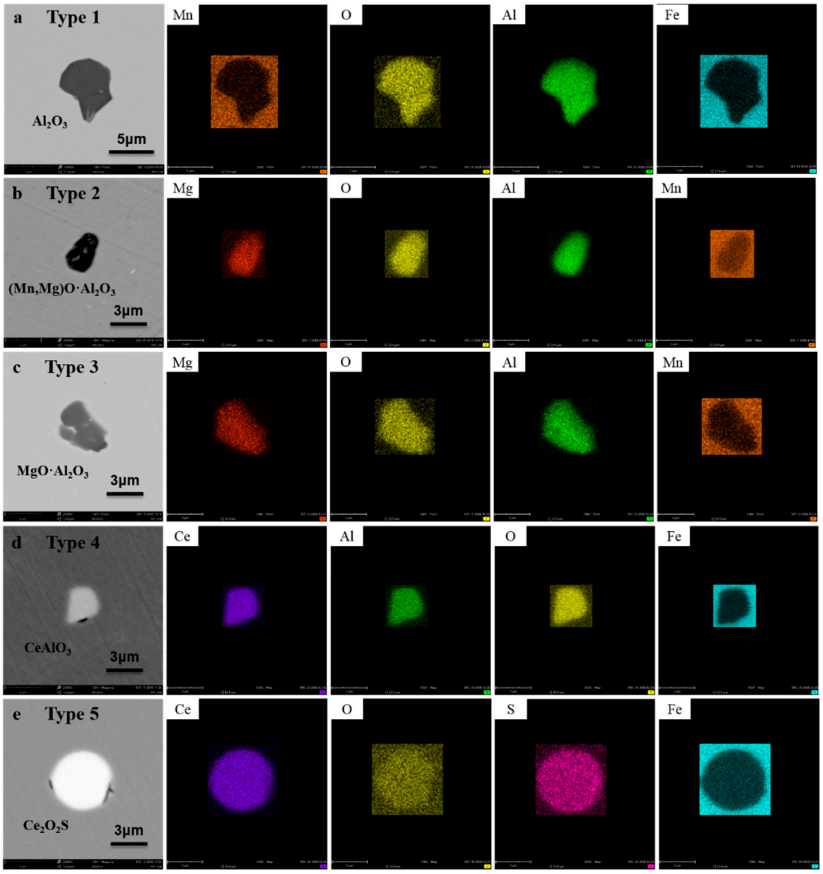

Figure 2. Elemental mapping of typical inclusions in steel: (**a**) Al_2O_3; (**b**) (Mn,Mg)O·Al_2O_3; (**c**) MgO·Al_2O_3; (**d**) $CeAlO_3$; (**e**) Ce_2O_2S.

After adding Ce, in addition to the above inclusions with uniform composition, there was a small amount of complex inclusions in the steel that underwent modification, as shown in Figure 3. In Figure 3a, the inclusion core is Mg-Al-O, and the outer layer is Ce-Al-O. In Figure 3b, the inclusion core is Mg-Al-O, and the outer layer is Ce-O-S. In Figure 3c, the inclusion is divided into three layers. The core is Mg-Al-O, the middle layer is Ce-Al-O, and the outermost layer is Ce-O-S. In Figure 3d, the inclusion core is Ce-O-S, and the outer layer is Ce-Al-O.

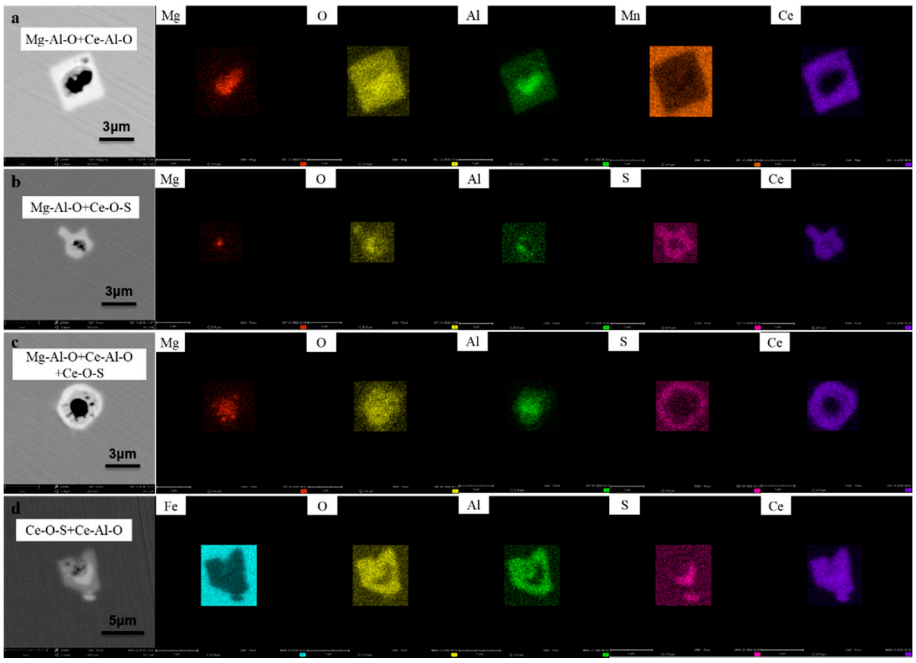

Figure 3. Elemental mapping of typical complex inclusions: (**a**) Mg-Al-O + Ce-Al-O; (**b**) Mg-Al-O + Ce-O-S; (**c**) Mg-Al-O + Ce-Al-O + Ce-O-S; (**d**) Ce-O-S + Ce-Al-O.

The types of uniform inclusions and complex inclusions for each sampling period are listed in Table 3. It can be seen that the inclusions in the three experimental steels were mainly spinel after aluminum deoxidation and magnesium treatment, and there was also a small amount of Al_2O_3 inclusions. The R1 experimental steel mainly contained (Mn,Mg)O·Al_2O_3 inclusions. The spinel inclusions in the R2 and R3 experimental steels were mainly MgO·Al_2O_3.

Table 3. Types of inclusions at different stages.

Type	Chemical Formula of Inclusions	Samples in R1 Steel				Samples in R2 Steel				Samples in R3 Steel			
		0	1	2	3	0	1	2	3	0	1	2	3
1	Al_2O_3	√				√				√			
2	(Mn,Mg)O·Al_2O_3	√√											
3	MgO·Al_2O_3	√				√√				√			
4	$CeAlO_3$		√√	√√	√√		√√	√	√				
5	Ce_2O_2S		√√	√			√√	√√	√√		√	√	√
a	Mg-Al-O + Ce-Al-O		√	√			√	√					
b	Mg-Al-O + Ce-O-S		√				√	√			√		
c	Mg-Al-O + Ce-Al-O + Ce-O-S		√				√				√		
d	Ce-O-S + Ce-Al-O			√									

Note: √√ represents the main type of inclusions, and √ represents a small number of inclusions.

After Ce treatment for 1 min, the inclusions in R1 experimental steel were mainly $CeAlO_3$ and Ce_2O_2S, and there was a small amount of complex inclusions of type a (Mg-Al-O + Ce-Al-O), b (Mg-Al-O + Ce-OS), and c (Mg-Al-O + Ce-Al-O + Ce-OS). After Ce treatment for 10 min, the inclusions

in steel were mainly $CeAlO_3$, while there was still a small amount of Ce_2O_2S inclusions as well as type a (Mg-Al-O + Ce-Al-O) and d (Ce-O-S + Ce-Al-O) complex inclusions. After Ce treatment for 30 min, the inclusions in the steel were almost all $CeAlO_3$. It indicated that Ce-Al-O and Ce-O-S inclusions would be directly formed in the steel after Ce addition. Meanwhile, spinel inclusions would also be modified by Ce. As time prolonged, spinel inclusions were gradually modified completely, and Ce-O-S would be transformed into Ce-Al-O.

After Ce treatment for 1 min, the inclusions in R2 experimental steel were mainly $CeAlO_3$ and Ce_2O_2S, and there was a small amount of complex inclusions of type a (Mg-Al-O + Ce-Al-O), b (Mg-Al-O + Ce-OS), and c (Mg-Al-O + Ce-Al-O + Ce-OS). After Ce treatment for 10 min, the inclusions in steel were mainly $CeAlO_3$, while there was still a small amount of Ce_2O_2S inclusions as well as type a (Mg-Al-O + Ce-Al-O) and b (Mg-Al-O + Ce-O-S) complex inclusions. After Ce treatment for 30 min, both $CeAlO_3$ and Ce_2O_2S were present in the steel. It indicated that Ce-Al-O and Ce-O-S inclusions would directly form in the steel after Ce addition. Meanwhile, spinel inclusions would also be modified by Ce. As time prolonged, spinel inclusions would gradually be transformed into Ce-Al-O and Ce-O-S.

After Ce treatment for 1 min, the inclusions in R3 experimental steel were mainly Ce_2O_2S, and there was a small amount of complex inclusions of type a (Mg-Al-O + Ce-Al-O) and c (Mg-Al-O + Ce-Al-O + Ce-OS). After Ce treatment for 10 min, the inclusions in steel were mainly Ce_2O_2S. It indicated that Ce-O-S inclusions would directly form in the steel after Ce addition. Meanwhile, spinel inclusions would also be modified by Ce. As time prolonged, spinel inclusions would be gradually transformed into Ce-O-S.

3.2. The Number Density and Size Change of Inclusions

In order to investigate the influence of Ce treatment on the number and size of inclusions in steel, Image pro plus software (Version 6.0, Media Cybernetics, Shanghai, China) was used to count the number density (number of inclusions per square millimeter) and size (equivalent diameter) of inclusions for each sampling period in the three experimental steels. Each sample counted 150 fields of view at 2000 magnification, for a total area of 1.5 mm^2. The number density and size change of inclusions during the experiment are shown in Figure 4.

It can be seen from Figure 4 that the variation law of the size and number density of inclusions in the three experimental steels is basically identical. After Ce treatment for 1 min, the proportion of inclusions with a size 0.5–2.0 μm (see Figure 4a) and the number density of inclusions (see Figure 4b) increased significantly. With the prolongation of treatment time, the number density of inclusions showed a decreasing trend, and the size of inclusions showed a slight increasing trend. However, inclusions with a size less than 5 μm were still dominant after 30 min.

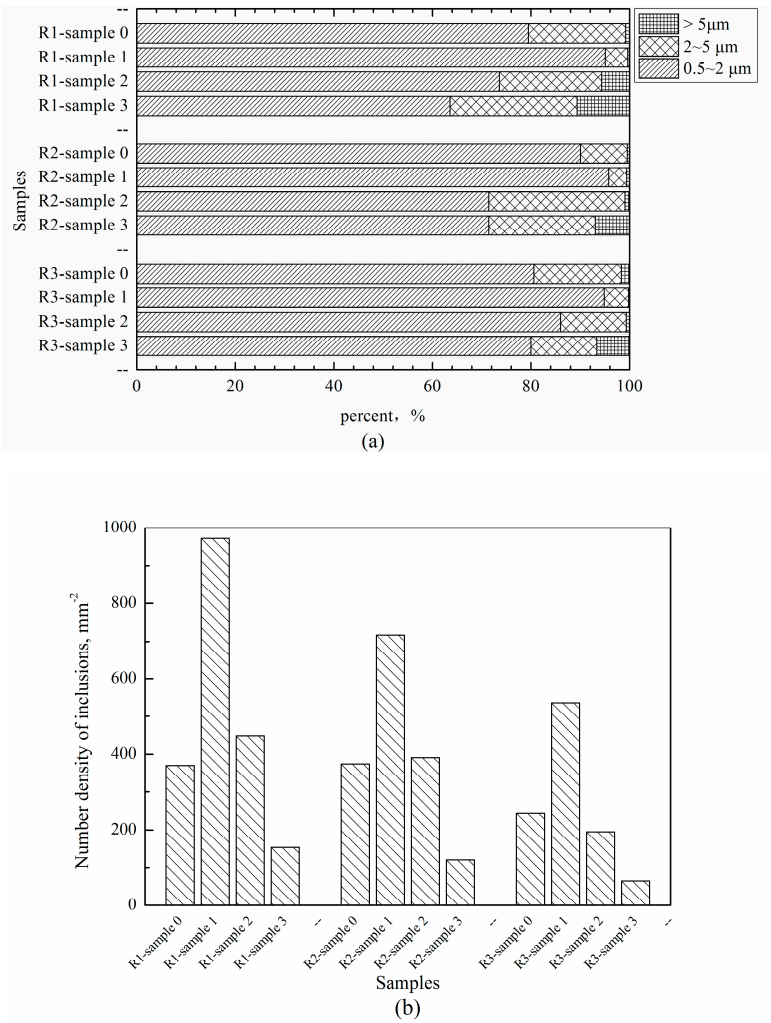

Figure 4. Size distribution (**a**) and number density (**b**) of inclusions in three steels at different stages.

4. Thermodynamics Analysis

After Ce treatment, the oxygen activity in the R1 experimental steel decreased (see Table 2), and the inclusions in the steel were mainly $CeAlO_3$ at 30 min after Ce treatment (see Table 3). The oxygen activity in R2 and R3 steels before Ce treatment had dropped to a very low level due to the high Al content. Therefore, the oxygen activity would not be further decreased after Ce addition (see Table 2). The inclusions present in the steels were mainly Ce_2O_2S at 30 min after Ce treatment, and only a small amount of $CeAlO_3$ inclusions were found in the R2 experimental steel (see Table 3). It indicates that Ce treatment can modify spinel inclusions into rare earth inclusions. The deoxidation reaction between Ce and O will preferentially proceed after the addition of Ce to steel, and Ce will react with S when the O content is at a very low level. The experimental phenomenon is consistent with previous research results [11,12].

To assess the evolution mechanism of inclusions in the steel, an inclusion stability diagram of Fe-10%Mn-0.001%Mg-0.015%S-0.015%Ce-Al-O system at 1873 K was calculated by FactSage^{TM} program (Version 7.1, developed by Thermfact/CRCT (Montreal, Canada) and GTT-Technologies (Achen, Germany)), as shown in Figure 5. The compositions of the three experimental steels are also marked in it. In the calculation, in addition to FactPS, FToxid, and FSstel databases, a privately created database MYDT containing thermodynamic data of Ce_2O_2S [13] was also selected. As can be seen from the figure, the stable inclusion region shows a change of $CeAlO_3 \rightarrow CeAlO_3 + Ce_2O_2S \rightarrow Ce_2O_2S$ as the oxygen content decreases within a fairly large range of Al content in the steel. The

composition of R1 experimental steel was located in the $CeAlO_3$ stable region, and the stable inclusions in the R2 experimental steel were $CeAlO_3$ + Ce_2O_2S, which was consistent with the experimental results (see Table 3). The thermodynamic calculation results of R3 experimental steel showed that there were no inclusions, which was inconsistent with the experimental results. The main reason is that thermodynamic calculations by Factsage have large deviations from the actual situation when the Al content is higher. This phenomenon is also proved by others [14], and a large amount of data indicate that the actual equilibrium oxygen content in steel is lower than the calculated value under high aluminum conditions in steel. Therefore, the activity relationship will be used to express the critical condition of inclusion transformation as follows.

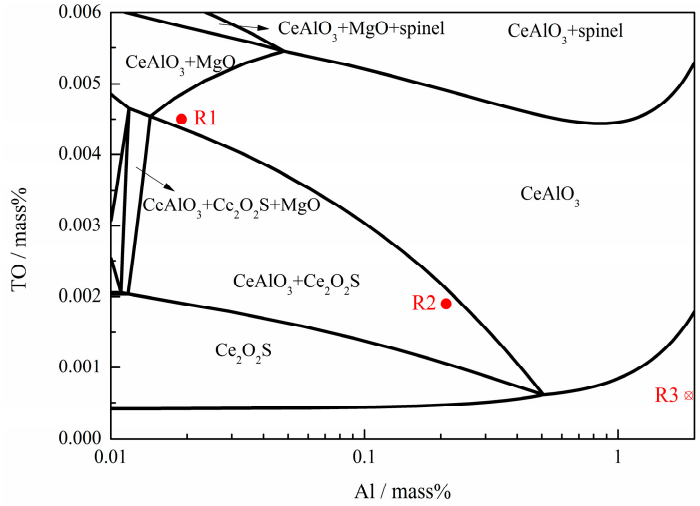

Figure 5. Stability diagram in the Fe-10%Mn-0.001%Mg-0.015%S-0.015%Ce-Al-O system at 1873 K.

According to the experimental results, the chemical reactions involved in the Fe-Mn-Al-Mg-Ce-O-S system and related standard Gibbs free energy [15–20] are shown in Table 4.

Table 4. Possible chemical reactions in steel and its standard Gibbs free energy.

No.	Reaction Equations in Molten Steel	ΔG^{θ} (J/mol)
1	$2[Al] + 3[O] = Al_2O_3(s)$	−867,370 + 222.5T [20]
2	$[Mg] + [O] = MgO(s)$	−89,960 − 82.0T [19]
3	$[Mn] + [O] = MnO(s)$	−287,900 + 125T [17]
4	$[Mn] + 2[Al] + 4[O] = MnO{\cdot}Al_2O_3(s)$	−1,545,000 + 524T [17]
5	$[Mg] + 2[Al] + 4[O] = MgO{\cdot}Al_2O_3(s)$	−978,182 + 128.93T [18]
6	$2[Ce] + 2[O] + [S] = Ce_2O_2S(s)$	−1,353,592.4 + 331.6T [16]
7	$[Ce] + [Al] + 3[O] = CeAlO_3(s)$	−1,366,460 + 364T [15]

The deoxidation equilibrium relationship of the molten steel includes Al-O, Al-Mg-O, Al-Ce-O, and Ce-S-O, and the formation conditions of the corresponding inclusions at 1873 K are as follows.

The formation condition of Al_2O_3 inclusions is that oxygen activity in steel is greater than that limited by the Al–O equilibrium, as shown in Equation (1)

$$a_O > a_{Al}^{-2/3} \cdot K_{Al_2O_3}^{-1/3} = 6.468 \times 10^{-5} \cdot a_{Al}^{-2/3}, \quad (1)$$

where K represents the equilibrium constant of the corresponding reaction, and a represents the activity of the corresponding component (the same as below).

The formation condition of $MgO{\cdot}Al_2O_3$ inclusions is that the actual oxygen activity in steel is greater than that limited by the Mg-Al-O equilibrium, as shown in Equation (2)

$$a_O > a_{Al}^{-1/2}{\cdot}a_{Mg}^{-1/4}{\cdot}K_{MgO{\cdot}Al_2O_3}^{-1/4} = 7.303\times10^{-6}{\cdot}a_{Al}^{-1/2}{\cdot}a_{Mg}^{-1/4}. \quad (2)$$

The formation conditions of $CeAlO_3$ inclusions is that the actual oxygen activity in steel is greater than that limited by Ce-Al-O equilibrium, as shown in Equation (3)

$$a_O > a_{Al}^{-1/3}{\cdot}a_{Ce}^{-1/3}{\cdot}K_{CeAlO_3}^{-1/3} = 4.31\times10^{-7}{\cdot}a_{Al}^{-1/3}{\cdot}a_{Ce}^{-1/3}. \quad (3)$$

The formation conditions of Ce_2O_2S inclusions is that the actual oxygen activity in steel is greater than that limited by Ce-O-S equilibrium, as shown in Equation (4)

$$a_O > a_{Ce}^{-1}{\cdot}a_S^{-1/2}{\cdot}K_{Ce_2O_2S}^{-1/2} = 6.1\times10^{-11}{\cdot}a_{Ce}^{-1}{\cdot}a_S^{-1/2}. \quad (4)$$

The transformation reaction between the inclusions can be obtained by associating the reactions in Table 2, as follows.

Conditions for Al_2O_3 transformation into $MgO{\cdot}Al_2O_3$:

$$4Al_2O_3(s) + 3[Mg] = 2[Al] + 3MgO{\cdot}Al_2O_3(s)\ \Delta G^\theta = 534,934 - 503.21T. \quad (5)$$

Let $\Delta G < 0$, at 1873 K:

$$a_{Mg} > 1.625\times10^{-4}{\cdot}a_{Al}^{2/3}. \quad (6)$$

Conditions for $MgO{\cdot}Al_2O_3$ transformation into $CeAlO_3$:

$$4[Ce] + 3MgO{\cdot}Al_2O_3(s) = 4CeAlO_3(s) + 3[Mg] + 2[Al]\ \Delta G^\theta = -2,531,294 + 1069.21T. \quad (7)$$

Let $\Delta G < 0$, at 1873 K:

$$a_{Ce} > 2.061\times10^{-4}{\cdot}a_{Mg}^{3/4}{\cdot}a_{Al}^{1/2}. \quad (8)$$

Conditions for $CeAlO_3$ transformation into Ce_2O_2S:

$$[Ce] + [S] + CeAlO_3(s) = Ce_2O_2S(s) + [Al] + [O]\ \Delta G^\theta = 12,867.6 - 32.4T. \quad (9)$$

Let $\Delta G < 0$, at 1873 K:

$$a_{Ce} > 0.0464{\cdot}a_O{\cdot}a_{Al}{\cdot}a_S^{-1}. \quad (10)$$

Conditions for $MgO{\cdot}Al_2O_3$ transformation into Ce_2O_2S:

$$8[Ce] + 4[S] + 3MgO{\cdot}Al_2O_3(s) = 4Ce_2O_2S(s) + 3[Mg] + 6[Al] + 4[O]\quad \Delta G^\theta = -2,479,823.6 + 939.61T. \quad (11)$$

Let $\Delta G < 0$, at 1873 K:

$$a_{Ce} > 3.09\times10^{-3}{\cdot}a_{Mg}^{3/8}{\cdot}a_{Al}^{3/4}{\cdot}a_O^{1/2}{\cdot}a_S^{-1/2}. \quad (12)$$

According to the above analysis, the inclusion formation conditions can be obtained as follows.

(1) The formation condition of $MgO{\cdot}Al_2O_3$ in steel at 1873 K after magnesium treatment needs to be considered from two different formation mechanisms, as above mentioned. One is that Al_2O_3 can transform into $MgO{\cdot}Al_2O_3$ (as shown in Equation (6)), which will provide a limit on magnesium activity. The other one is that $MgO{\cdot}Al_2O_3$ can directly form from steel (as shown in Equation (2)), which requires the oxygen activity to be higher than the equilibrium oxygen activity limited by Mg-Al-O, as follows.

$$a_{Mg} > 1.625\times10^{-4}{\cdot}a_{Al}^{2/3},\ a_O > 7.303\times10^{-6}{\cdot}a_{Al}^{-1/2}{\cdot}a_{Mg}^{-1/4}. \quad (13)$$

(2) There are also two considerations for the formation condition of single $CeAlO_3$ in steel at 1873 K. One is that $MgO{\cdot}Al_2O_3$ can transform into stable $CeAlO_3$ (as shown in Equation (8)), which means $CeAlO_3$ cannot spontaneously transform into Ce_2O_2S (as shown in Equation (10)); this will provide both the upper and lower limits of Ce activity. The other consideration is that $CeAlO_3$ can directly form from steel (as shown in Equation (3)), but Ce_2O_2S should not spontaneously precipitate (as shown in Equation (4)). This will also limit the upper and lower limits of oxygen activity, which means the oxygen activity should be higher than the equilibrium oxygen activity limited by Ce-Al-O but lower than the equilibrium oxygen activity limited by Ce-O-S, as follows.

$$\begin{gathered} 0.0464{\cdot}a_{\mathrm{O}}{\cdot}a_{\mathrm{Al}}{\cdot}a_{\mathrm{S}}^{-1} > a_{\mathrm{Ce}} > 2.061\times10^{-4}{\cdot}a_{\mathrm{Mg}}^{-3/4}{\cdot}a_{\mathrm{Al}}^{-1/2}, \\ 6.1\times10^{-11}{\cdot}a_{\mathrm{Ce}}^{-1}{\cdot}a_{\mathrm{S}}^{-1/2} > a_{\mathrm{O}} > 4.31\times10^{-7}{\cdot}a_{\mathrm{Al}}^{-1/3}{\cdot}a_{\mathrm{Ce}}^{-1/3}. \end{gathered} \tag{14}$$

(3) There are also two considerations for the formation condition of $CeAlO_3$ and Ce_2O_2S in steel at 1873 K. One is that $MgO{\cdot}Al_2O_3$ can transform into stable $CeAlO_3$ (as shown in Equation (8)), and $CeAlO_3$ can transform into Ce_2O_2S (as shown in Equation (10)); this will provide both the lower limits of Ce activity. The other consideration is that $CeAlO_3$ and Ce_2O_2S can directly form from steel (as shown in Equations (3) and (4)). This will also limit the lower limits of oxygen activity, which means the oxygen activity should be higher than the equilibrium oxygen activity limited by Ce-Al-O and Ce-O-S, as follows.

$$\begin{gathered} a_{\mathrm{Ce}} > \max\left\{2.061\times10^{-4}{\cdot}a_{\mathrm{Mg}}^{3/4}{\cdot}a_{\mathrm{Al}}^{1/2}, 3.09\times10^{-3}{\cdot}a_{\mathrm{Mg}}^{3/8}{\cdot}a_{\mathrm{Al}}^{3/4}{\cdot}a_{\mathrm{O}}^{1/2}{\cdot}a_{\mathrm{S}}^{-1/2}\right\}, \\ a_{\mathrm{O}} > \max\left\{4.31\times10^{-7}{\cdot}a_{\mathrm{Al}}^{-1/3}{\cdot}a_{\mathrm{Ce}}^{-1/3}, 6.1\times10^{-11}{\cdot}a_{\mathrm{Ce}}^{-1}{\cdot}a_{\mathrm{S}}^{-1/2}\right\}. \end{gathered} \tag{15}$$

(4) There are also two considerations for the formation condition of single Ce_2O_2S in steel at 1873 K. One is that $MgO{\cdot}Al_2O_3$ can transform into stable Ce_2O_2S (as shown in Equation (10)), which means $CeAlO_3$ cannot spontaneously transform into $CeAlO_3$ (as shown in Equation (8)); this will provide both the upper and lower limits of Ce activity. The other consideration is that Ce_2O_2S can directly form from steel (as shown in Equation (4)), but $CeAlO_3$ should not spontaneously precipitate (as shown in Equation (3)). This will also limit the upper and lower limits of oxygen activity, which means the oxygen activity should be higher than the equilibrium oxygen activity limited by Ce-O-S but lower than the equilibrium oxygen activity limited by Ce-Al-O, as follows.

$$a_{\mathrm{Ce}} > 3.09\times10^{-3}{\cdot}a_{\mathrm{Mg}}^{3/8}{\cdot}a_{\mathrm{Al}}^{3/4}{\cdot}a_{\mathrm{O}}^{1/2}{\cdot}a_{\mathrm{S}}^{-1/2},\ 4.31\times10^{-7}{\cdot}a_{\mathrm{Al}}^{-1/3}{\cdot}a_{\mathrm{Ce}}^{-1/3} > a_{\mathrm{O}} > 6.1\times10^{-11}{\cdot}a_{\mathrm{Ce}}^{-1}{\cdot}a_{\mathrm{S}}^{-1/2}. \tag{16}$$

In summary, the modification mechanism of Ce to spinel inclusions can be shown in Figure 6. Ce can modify the spinel inclusions into $CeAlO_3$ or Ce_2O_2S. There are three main modification paths: ① Spinel can directly transform into $CeAlO_3$ by Ce, namely spinel → Ce-Al-O + Mg-Al-O → $CeAlO_3$, which can be proved by the complex inclusion shown in Figure 3a. ② After Ce treatment, spinel can be preferentially transformed to $CeAlO_3$. After a while, the resulting $CeAlO_3$ product layer will be transformed to Ce_2O_2S. The first-step reaction was considered to be difficult to perform completely because we observed some inclusions with a three-layer structure in the experiment, as shown in Figure 3c. If treatment time is enough, it will eventually transform into uniform Ce_2O_2S. The above path can be summarized as spinel → Ce-Al-O + Mg-Al-O → Ce-O-S + Ce-Al-O + Mg-Al-O → Ce_2O_2S. ③ Spinel can be directly transformed into Ce_2O_2S by Ce, the modification path is spinel → Ce-O-S + Mg-Al-O → Ce_2O_2S. The related modification mechanism is as follows: After Ce addition, Mn and Mg in the spinel inclusions are first replaced by Ce, and the spinel structure will be destroyed in the above process to form $CeAlO_3$. If the O content in the steel is low, which means that the S content is relatively high, S in the steel will participate in the above displacement reaction to replace the O in the inclusion. In general, $CeAlO_3$ and spinel inclusions will transform into Ce_2O_2S through paths 2 and 3. Under the experimental steel conditions, the modification sequence of Ce to spinel inclusions is spinel → $CeAlO_3$ → Ce_2O_2S.

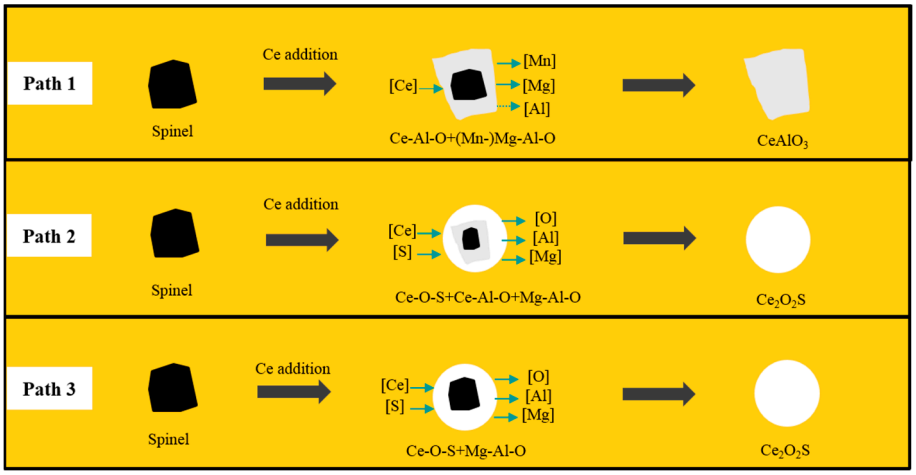

Figure 6. Modification mechanism of spinel inclusions.

Huang et al. [7,9] and Wang et al. [8] reported that the sequence of Ce-modified spinel is spinel → $CeAlO_3$ → Ce_2O_3 → Ce_2O_2S or spinel → Ce_2O_3 → Ce_2O_2S. However, no Ce_2O_3 inclusions were found in the present experimental steel. After comparing the experimental conditions, it was found that the contents of Al and S in the steel were different. Therefore, the stability diagram in the Fe-10%Mn-0.001%Mg-0.015%Ce-0.005%O-Al-S system at 1873 K was calculated using FactSage 7.1 (databases FactPS, FToxid, FSstel, MYDT), as shown in Figure 7. As can be seen from the red line in Figure 7, as the S content in the steel increased, the precipitation condition for the Ce_2O_3 required a lower Al content. The S content in our experimental steels was as high as 0.015%. Therefore, the formation condition of Ce_2O_3 was not reached when the Al content was higher than 0.02%.

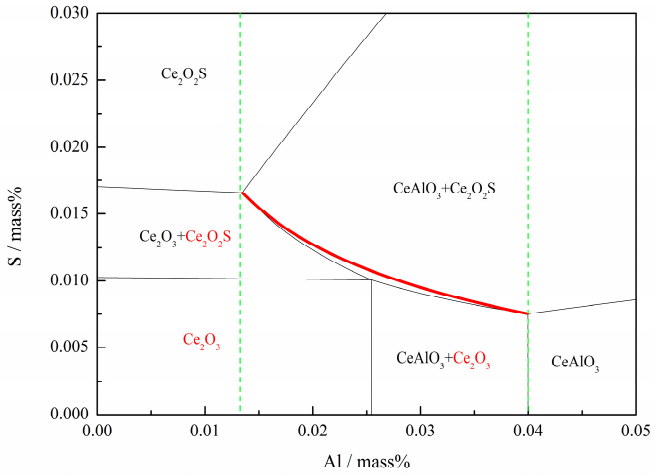

Figure 7. Stability diagram in the Fe-10%Mn-0.001%Mg-0.015%Ce-0.005%O-Al-S system at 1873 K.

5. Ce Content Required for Complete Modification of Spinel Inclusions

There are complex interactions between different elements, such as Ce, Al, O, and S, in the steel during the modification process. Under present experimental conditions, spinel is preferentially transformed to $CeAlO_3$. In order to obtain the minimum Ce content required for complete modification of spinel inclusions, the effect of aluminum and oxygen content on the related Ce content in steel was calculated by FactSage. The content of each element in the steel discussed in this section is total content, and the calculation results are shown in Figure 8.

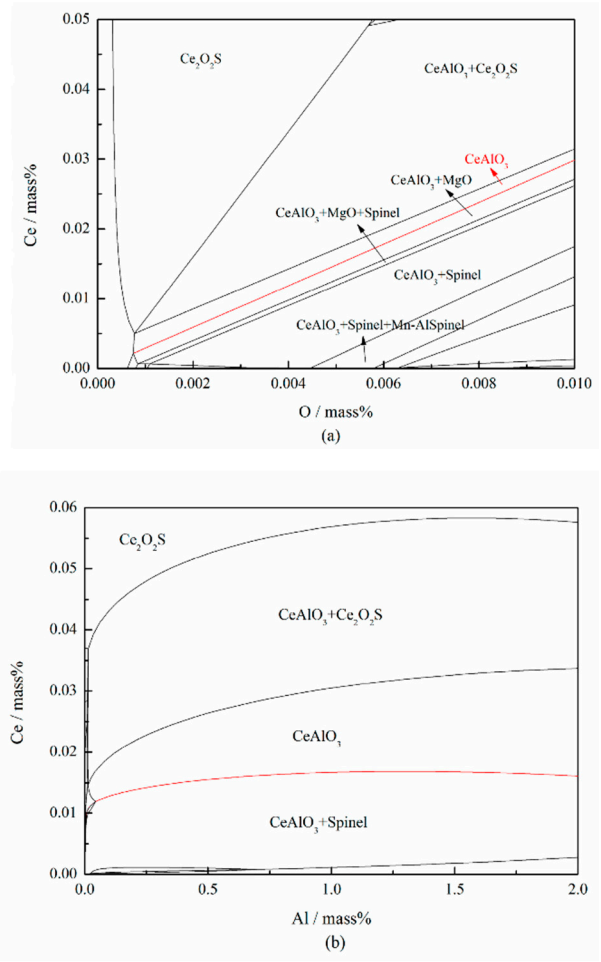

Figure 8. Effect of oxygen and aluminum content on inclusions in steel, (**a**) w_S = 0.015% and w_{Al} = 0.02%, (**b**) w_O = 0.0045% and w_S = 0.015%.

Figure 8a shows the effect of oxygen content on inclusions in steel, where w_{Al} = 0.02% and w_S = 0.015%. It can be seen from the red line in the figure that the minimum Ce content required for modification of spinel inclusions is linear with the oxygen content in the steel. When $w_{Ce} = 2.99 \cdot w_O$, the inclusions in the steel can be controlled as $CeAlO_3$. Wang et al. [8] also obtained a similar conclusion: that increasing the O content would increase the Ce content required for complete modification of spinel inclusions.

Theoretically, the inclusions can be controlled to be $CeAlO_3$ when the Ce content in the steel is three times that of the oxygen content. Therefore, by measuring the oxygen content in the steel, a suitable rare earth Ce addition amount required for complete modification of spinel inclusions can be obtained.

Figure 8b shows the effect of aluminum content on types of stable inclusions in steel, where w_O = 0.0045% and w_S = 0.015%. It can be seen from the red line in the figure that as the aluminum content in the steel increases, the minimum Ce content required for modification spinel inclusions does not change much, which indicates that the aluminum content has little effect on the minimum Ce content required for modification of spinel inclusions.

6. Conclusions

In present paper, the transformation process of inclusions in medium manganese steel was studied by high-temperature simulation experiments. The modification mechanism of inclusions in steel under different aluminum contents was discussed by thermodynamic calculations. Under the present experimental conditions, the following conclusions were obtained.

(1) Ce treatment can modify spinel inclusions into rare earth inclusions. After Ce treatment, the amount of inclusions in the steel will decrease, and the size of inclusions is basically less than 5 μm.

(2) The modification mechanism of spinel inclusions by Ce is as follows: After Ce is added to steel, Mn and Mg in the spinel inclusions are first replaced by Ce to form $CeAlO_3$, which will cause the destruction of the spinel structure. When the O content in the steel is at a lower level, S in the steel will take part in the replacement reaction to replace the O in the inclusion, then the $CeAlO_3$ and spinel inclusions will be finally transformed into Ce_2O_2S.

(3) In the Fe-Mn-Al-Mg-Ce-O-S system at 1873 K, the conditions for forming single $CeAlO_3$ are $0.0464 \cdot a_O \cdot a_{Al} \cdot a_S^{-1} > a_{Ce} > 2.061 \times 10^{-4} \cdot a_{Mg}^{3/4} \cdot a_{Al}^{1/2}$, $6.1 \times 10^{-11} \cdot a_{Ce}^{-1} \cdot a_S^{-1/2} > a_O > 4.31 \times 10^{-7} \cdot a_{Al}^{-1/3} \cdot a_{Ce}^{-1/3}$; the conditions for simultaneous formation of $CeAlO_3$ and Ce_2O_2S are $a_{Ce} > \max\left\{2.061 \times 10^{-4} \cdot a_{Mg}^{3/4} \cdot a_{Al}^{1/2}, 3.09 \times 10^{-3} \cdot a_{Mg}^{3/8} \cdot a_{Al}^{3/4} \cdot a_O^{1/2} \cdot a_S^{-1/2}\right\}$, $a_O > \max\left\{4.31 \times 10^{-7} \cdot a_{Al}^{-1/3} \cdot a_{Ce}^{-1/3}, 6.1 \times 10^{-11} \cdot a_{Ce}^{-1} \cdot a_S^{-1/2}\right\}$; and the conditions for forming single Ce_2O_2S are $a_{Ce} > 3.09 \times 10^{-3} \cdot a_{Mg}^{3/8} \cdot a_{Al}^{3/4} \cdot a_O^{1/2} \cdot a_S^{-1/2}$, $4.31 \times 10^{-7} \cdot a_{Al}^{-1/3} \cdot a_{Ce}^{-1/3} > a_O > 6.1 \times 10^{-11} \cdot a_{Ce}^{-1} \cdot a_S^{-1/2}$.

(4) The minimum Ce content required for complete modification of spinel inclusions is mainly related to the O content. When the total Ce content is three times that of the total O content in the steel, the spinel inclusions can be transformed into $CeAlO_3$.

Author Contributions: Z.X. and C.L. conceived and designed the experiments, analyzed the data, and conducted writing–original draft preparation, editing, and visualization.

Funding: This work was financially supported by the National Key R&D Program of China (No. 2017YFC0805100), the National Natural Science Foundation of China (No. 51874082), and the Fundamental Research Funds for the Central Universities (Grant No. N180725008).

Acknowledgments: Thanks to Jiyu Qiu for providing language help.

Conflicts of Interest: The authors declare no conflict of interest.

References

1. Kong, L.Z.; Deng, Z.Y.; Zhu, M.Y. Formation and evolution of non-metallic inclusions in medium Mn steel during secondary refining process. *ISIJ Int.* **2017**, *57*, 1537–1545. [CrossRef]
2. Shao, X.J.; Ji, C.X.; Cui, Y.; Li, H.B.; Zhu, G.S.; Chen, B.; Liu, B.S.; Bao, C.L. Brief instruction of the effect of inclusions on fatigue behavior of steel. In Proceedings of the National Steelmaking Conference, Xi'an, China, 21 May 2014.
3. Wang, L.; Zhang, P.J.; Lu, J.X. Quality and production technology of steel sheets for automobile. *Iron Steel* **1999**, *34*, 908–912. (In Chinese)
4. Yang, S.F.; Li, J.S.; Wang, Z.F.; Li, J.; Lin, L. Modification of $MgO \cdot Al_2O_3$ spinel inclusions in Al-killed steel by Ca-treatment. *Int. J. Miner. Metall. Mater.* **2011**, *18*, 18–23. [CrossRef]
5. Pretorius, E.B.; Oltmann, H.G.; Cash, T. The effective modification of spinel inclusions by Ca treatment in LCAK steel. *Iron Steel Technol.* **2010**, *7*, 31–44.
6. Ma, W.J.; Bao, Y.P.; Wang, M.; Zhao, L.H. Effect of Mg and Ca treatment on behavior and particle size of inclusions in bearing steels. *ISIJ Int.* **2014**, *54*, 536–542. [CrossRef]
7. Huang, Y.; Cheng, G.G.; Xie, Y. Modification mechanism of cerium on the inclusions in drill steel. *Acta Metall.* **2018**, *54*, 1253–1261.
8. Wang, L.J.; Liu, Y.Q.; Chou, K.C. Evolution mechanisms of $MgO \cdot Al_2O_3$ inclusions by cerium in spring steel used in fasteners of high-speed railway. *Trans. Iron Steel Inst. Jpn.* **2015**, *55*, 970–975. [CrossRef]
9. Huang, Y.; Cheng, G.G.; Li, S.J.; Dai, W.X. Effect of Cerium on the Behavior of Inclusions in H13 Steel. *Steel Res. Int.* **2018**, *89*, 1800371. [CrossRef]
10. Hirata, H.; Isobe, K. Steel having finely dispersed inclusions. U.S. Patent 20060157162A1, 20 July 2006.
11. Adabavazeh, Z.; Hwang, W.S.; Su, Y.H. Effect of adding cerium on microstructure and morphology of Ce-based inclusions formed in low-carbon steel. *Sci. Rep.* **2017**, *7*, 1–10. [CrossRef] [PubMed]
12. Wilson, W.G.; Kay, D.A.R.; Vahed, A. The use of thermodynamics and phase equilibria to predict the behavior of the rare earth elements in steel. *JOM* **1974**, *26*, 14–23. [CrossRef]

13. Fruehan, R.J. The free energy of formation of Ce_2O_2S and the nonstoichiometry of cerium oxides. *Metall. Mater. Trans. B* **1979**, *10*, 143–148. [CrossRef]
14. Paek, M.K.; Jang, J.M.; Kang, Y.B.; Pak, J.J. Aluminum deoxidation equilibria in liquid iron: Part I. experimental. *Metall. Mater. Trans. B* **2015**, *46*, 1826–1836. [CrossRef]
15. Vahed, A.; Kay, D.A.R. Thermodynamics of rare earths in steelmaking. *Metall. Mater. Trans. B* **1976**, *7*, 375–383. [CrossRef]
16. Du, T. Thermodynamics of rare earth elements in iron-base solutions. *J. Iron. Steel Res.* **1994**, *6*, 6–12.
17. Hong, T.; Debroy, T. Time-temperature-transformation diagrams for the growth and dissolution of inclusions in liquid steels. *Scr. Mater.* **2001**, *44*, 847–852. [CrossRef]
18. Itoh, H.; Hino, M.; Ban, Y.S. Thermodynamics on the formation of non-metallic inclusion of spinel ($MgO{\cdot}Al_2O_3$) in liquid steel. *Tetsu-to-Hagané* **1998**, *84*, 85–90. [CrossRef]
19. Rohde, L.E.; Choudhury, A.; Wahlster, M. Neuere Untersuchungen über das Aluminium-Sauerstoff-Gleichgewicht in Eisenschmelzen. *Archiv für das Eisenhüttenwesen* **1971**, *42*, 165–174. [CrossRef]
20. Seo, J.D.; Kim, S.H.; Lee, K.R. Thermodynamic assessment of the Al deoxidation reaction in liquid iron. *Steel Res. Int.* **1998**, *69*, 49–53. [CrossRef]